MATHEMATICAL MODELING AND COMPUTING, Vol. 9, No. 2, pp. 203–216 (2022)

Field scale computer modeling of soil moisture with dynamic nudging assimilation algorithm

Kozhushko O. D.[1,2], Boiko M. V.[1,2], Kovbasa M. Yu.[3],
Martyniuk P. M.[1,2], Stepanchenko O. M.[1,2], Uvarov N. V.[1,4]

[1] *EOS Data Analytics,*
5 Desyatynnyi Ln., 01025, Kyiv, Ukraine
[2] *National University of Water and Environmental Engineering,*
11 Soborna Str., 33028, Rivne, Ukraine
[3] *V. Ye. Lashkaryov Institute of Semiconductor Physics of the National Academy of Sciences of Ukraine,*
41 Nauky Ave., 03028, Kyiv, Ukraine
[4] *G. V. Kurdyumov Institute for Metal Physics of the National Academy of Sciences of Ukraine,*
36 Acad. Vernadsky Blvd., 03142, Kyiv, Ukraine

(Received 13 August 2021; Accepted 7 February 2022)

Soil moisture analysis is widely used in numerous practical cases, from weather forecasts to precise agriculture. Recently, availability of moisture data increased due to the rapid development of satellite image processing. However, satellite retrievals mostly provide low-resolution surface data. In this study, we attempt to retrieve surface soil moisture on the field scale using a decomposition algorithm. Furthermore, we add a mathematical model based on Richards equation to evaluate soil moisture in the root zone. To combine the results of both models, we employ a nudging data assimilation technique. Also, a dynamical variation of the method is proposed which makes it more adaptive to the soil type and provides improvement to modeling results. Two types of numerical experiments are conducted. Simulation results show reasonably good convergence with the measurements. The model performs with average correlation of 0.58 on the whole root zone, reaching 0.85 on top soil layers.

Keywords: *data assimilation, Earth remote sensing, Newtonian nudging algorithm, computer modeling, satellite moisture retrieval, soil moisture.*

2010 MSC: 35K20, 35Q35, 65M06, 68U10, 76M20 **DOI:** 10.23939/mmc2022.02.203

1. Introduction

Soil moisture is one of the crucial variables for land and atmosphere system modeling. Precise and up-to-date information on soil moisture is required for real-world applications such as water resource management, runoff and flood prediction, weather and climate forecasting. In agriculture, knowledge of current soil moisture conditions enables better yield prediction, irrigation planning, and water conservation. It obviously finds a great use in agriculture and can enhance its sustainable development; however, these applications demand frequent and accurate monitoring. Ground observations may be the most accurate source of soil moisture data, but they are relatively expensive and provide only sparse local information.

In the last decades, satellite imagery became acknowledged as an effective and accessible alternative for ground observations. Microwave sensors are able to provide soil moisture measurements over large spatial scales with reasonable accuracy. As the quality and availability of satellite retrievals is improving, their use in land monitoring is growing. However, satellite retrievals reflect only the state of the top soil layer ($0-5\,\text{cm}$) and at isolated instances of time, which is often not enough to describe the state of the entire system.

A variety of methods is developed to propagate satellite observations onto continuous problem domain. For example, exponential filters can provide estimates on root zone soil moisture based

on satellite-retrieved values. This approach is rather effective for its simplicity, yet receives mixed validation results from researchers. Some mark its ability of predicting the patterns [1], and others show the quality of exponential filters results is still not as good as land surface model predictions [2,3]. It can also be expected that these results must depend greatly on the quality of observations, since the errors present in retrievals are propagated further.

Land surface models, on the other hand, are able to provide continuous predictions of the system state, but they contain errors due to multiple generalizations of process physics. In addition, as shown in [4], simulated soil moisture is highly dependent on chosen model and parameters, and so cannot represent real state precisely, especially at field scale. Therefore, a model can benefit greatly from the satellite data, and combining them is a powerful tool for improving the quality of predictions. One way is to do that is to use Earth remote sensing data for model calibration and parameter estimation. This has been implemented successfully, for example, in [5–7]. The other way is to include observations into the problem solving process, thus adapting the model output to observed real state. The latter approach is known as data assimilation, and is popular in many modeling branches including hydrology. Also, some recent studies combine both uses, updating both state and parameter estimates with observations [8, 9].

Data assimilation involves combining data from different sources on the same variable, such as soil moisture predicted by model, observed by satellite or ground sensors. While both the model and observations are imperfect, they contain different kinds of information, and so their combination is able to yield more accurate result than each of them does separately [10]. Such assimilated results agree better with the real state of the system than each of the sources alone, which has been proved in a number of works [11–13]. Some studies aimed at measuring the positive impact of combining observations with a model, e.g. [11, 14, 15] to name a few.

Assimilation of satellite soil moisture has been successfully used in numerous land surface models. GLDAS [16] and CLM [17, 18] might be the most notable examples of this. Studies [9, 19–25] are just a few cases from the multitude of other recent implementations. Soil moisture assimilation also allows solving more complex problems that require additional data, such as inverse problems or rainfall correction [26].

Basically, data assimilation methods can be divided in two main categories: smoothing and filtering. Filtering works in a predictor-corrector scheme, where the simulated state is first evaluated by the model and then corrected (filtered) based on the observations. Common examples are popular Kalman filters (KF), but also three dimensional variational assimilation (3D-Var) and particle filters should be noted. Smoothing methods, on the other hand, add observations into the model continuously, combining past and future information [10]. This category includes 4D-Var and its parent, Newtonian relaxation or nudging.

Newtonian nudging (NN) has first been used for meteorology and oceanography problems to refine initial conditions. Later it received application in hydrology problems, not least in soil moisture prediction. NN has been used in a number of global and regional scale models, such as GLEAM, TOPLATS and CATCHY [27–29]. The method involves adding a nudging term into the model equation, which can be physically interpreted as a force pulling the solution towards observations.

A number of studies investigated the relation of NN to other assimilation methods. For example, Vidard et al. [30] proposed a formulation of NN similar to 4D-Var and KF. Results of [31] indicate that KF generally performs better than NN, but the latter is more effective computationally. For that reason, in GLEAM v.3 Kalman filters were replaced with NN, yielding results of nearly the same accuracy for much less computational time [27]. It has also been reasoned from theoretical point of view that the principal concept of smoothing methods like NN and 4D-Var better suits continuous problems than KF, since filtering corrections can cause model shocks [10]. Most recent researches successfully implemented ensemble Kalman filter to Richards equation-based models in spite of the reported difficulties, see for example [32, 33]. Still, a more stable and cheaper NN method is still preferred in complex nonlinear problems, e.g. unsteady water flow problems as described in [34].

The purpose of this study is to develop a complex model for simulating soil moisture with both satellite and land model level, which will be able to predict soil moisture at field scale. Section 2 of the paper deals with the core of the mathematical model. Section 3 explains adjustments made to the Newtonian nudging method in the moisture governing equation. Section 4 describes the procedure used to acquire satellite retrievals. Section 5 contains verification setting and discussion.

2. Mathematical model and numerical solving process

We use Richards equation-based model to describe subsurface water flow. It is a well-known and consistent approach for soil moisture flow problems, used, for example, in HYDRUS [35,36], CATCHY [28,32] and other models, e.g. [33, 37]. We also include the heat transfer equation into our model, since heat has influence on water flow in the soil and vice versa. Moreover, soil temperature is another variable that can be retrieved from satellite images and assimilated. Here we implement the thermally induced water flux theory by Philip and de Vries [38]. Other associated processes like salinity or vapor flow are neglected in the current model, but may be studied in the future. Our model consists of coupled nonlinear moisture transport and heat transfer boundary value problem. We assume a one-dimensional soil layer of thickness l and downward x axis, with $x = 0$ at the soil surface. Then the corresponding problem settings are as follows:

$$\frac{\partial\theta(x,t)}{\partial t} = \frac{\partial}{\partial x}\left(k(h)\frac{\partial h}{\partial x} - k_T\frac{\partial T}{\partial x}\right) - \frac{\partial k(h)}{\partial x} - S_{\mathrm{rwu}}(h,x,t), \tag{1}$$

$$\left(k(h)\frac{\partial h}{\partial x} - k(h)\right)\Big|_{x=0} = Q(t) - E_s(t), \quad t \geqslant 0, \tag{2}$$

$$\frac{\partial h}{\partial x}\Big|_{x=l} = 0, \quad t \geqslant 0, \tag{3}$$

$$h(x,0) = h_0(x), \quad x \in [0;l]; \tag{4}$$

$$c_T\frac{\partial\theta(x,t)}{\partial t} = \frac{\partial}{\partial x}\left(\lambda(h)\frac{\partial T}{\partial x}\right) - \rho c_w u(h)\frac{\partial\theta(x,t)}{\partial x}, \tag{5}$$

$$T(x,t)|_{x=0} = T_1(t), \quad t \geqslant 0, \tag{6}$$

$$T(x,t)|_{x=l} = T_2(t), \quad t \geqslant 0, \tag{7}$$

$$T(x,0) = T_0(x), \quad x \in [0;l]. \tag{8}$$

Here θ is absolute soil moisture, h is pressure head, T is temperature, k is soil hydraulic conductivity, k_T is hydraulic conductivity due to temperature, $S_{\mathrm{rwu}}(h,x,t)$ is root water uptake, $\lambda(h)$ is soil thermal conductivity, $c_T = c_n(1-\theta) + c_w\theta$ is volumetric heat capacity of porous medium, c_n and c_w are specific heat capacity of solid soil and water, respectively, ρ is soil water density, $u(h)$ is soil water flux rate. In the boundary conditions, $Q(t)$ is precipitation rate, $E_s(t)$ is soil evaporation rate, $T_1(t)$ and $T_2(t)$ are temperatures on the soil surface and l m depth; $h_0(x)$ and $T_0(x)$ are initial conditions for pressure head and temperature, respectively.

Among the most notable problems associated with Richards equation is the choice of relations between moisture and pressure head, since both are present in the equation. In our model, we use Mualem–van Genuchten model [39], represented by the following equations:

$$\theta(h) = \theta_{min} + \frac{\theta_{max} - \theta_{min}}{(1 + (-\alpha h)^n)^m}, \quad m = 1 - \frac{1}{n}, \tag{9}$$

$$k(h) = k_s S^l\left(1 - \left(1 - S^{\frac{1}{m}}\right)^m\right)^2, \tag{10}$$

where θ_{min} and θ_{max} are residual (minimum) and saturation (maximum) water content, k_s is saturated soil hydraulic conductivity, $S = (\theta - \theta_{min})/(\theta_{max} - \theta_{min})$ is saturation degree, α, n and l are empirical model parameters. These relations are well-established and widely used in Richards-based models,

including the ones cited above. Many studies are dedicated to evaluation of Mualem–van Genuchten model parameters, among which program estimators like Rosetta [40] should be noted.

Hence, considering equations (9), (10) soil moisture state equation (1) can be transformed to the following form with the only unknown state variable — pressure head:

$$\beta(h)\frac{\partial h}{\partial t} = \frac{\partial}{\partial x}\left(k(h)\frac{\partial h}{\partial x} - k_T\frac{\partial T}{\partial x}\right) - v(h)\frac{\partial h(x,t)}{\partial x} - S_{\text{rwu}}(h,x,t), \tag{11}$$

where values of coefficients $\beta(h) = \frac{\partial\theta}{\partial h}$, $v(h) = \frac{\partial k(h)}{\partial h}$ can be calculated analytically according to Mualem–van Genuchten model.

We also account for nonlinearity of heat equation coefficients, namely, $\lambda(h)$ and c_T. Sadeghi et al. [41] describe numerous relations for thermal conductivity $\lambda(\theta)$. In our model, we make use of Chung and Horton model:

$$\lambda_0(\theta) = b_1 + b_2\theta + b_3\sqrt{\theta}, \tag{12}$$

where b_1, b_2, b_3 are empirical parameters.

Evaporation and crop water uptake (connected to the transpiration) terms depend on weather and vegetation. Potential evaporation can be calculated by the means meteorological parameters [42], and is also provided by some weather services. Root water uptake is limited by potential evapotranspiration and water availability, as expressed in the Feddes model, see [43] for reference.

The described one-dimensional problem can be solved on a uniform grid with a finite difference scheme. Both moisture (11), (2)–(4) and heat transport (5)–(8) problems are solved consecutively on each discrete time step. Particularly, we employ a homogeneous difference scheme that is intended for equations with variable coefficients [44]. However, coefficients calculated by Mualem–van Genuchten relations are not only variable, but nonlinear, which presents additional computational difficulties. To deal with nonlinearity, we implement an implicit iterative scheme proposed by Samarskiy. The scheme requires additional iterations on each time step, but allows solving nonlinear problems without further transformation of model equation, e.g. by Newton linearization method. The iterative scheme is guaranteed to converge and in practice yields stable result even with considerably large time step [44].

3. Newtonian nudging assimilation

In spite of many good data assimilation practices suggested in the literature, only some of them can be readily applied to solving boundary value problems, since their solution has a much more complicated structure than time series. Assimilating observations, which affects only part of the problem domain, can disrupt the numerical scheme and lead to instabilities. Therefore, we chose Newtonian nudging for its simplicity and stability. Another advantage of NN is that the nudging process is included directly into the model equation. Thus, we are guaranteed that the solving process is not disrupted by assimilated observations, and the solution agrees with our linearization scheme on each iteration.

The nudging method consists in adding the so-called nudging term to the Richards equation:

$$\frac{\partial\theta}{\partial t} = \frac{\partial}{\partial x}\left(k(h)\frac{\partial h}{\partial x} - k(h)\right) - S_{\text{rwu}}(h,x,t) + G\,W(x,t)\,\varepsilon(x)\,(\theta_{\text{obs}} - \theta)\,, \tag{13}$$

where θ_{obs} is observed surface soil moisture, G is nudging factor, $W(x,t)$ is weight function, and $\varepsilon(x)$ is called degree of trust or accuracy of observations. Note that, thought the final form (11) is written in pressure heads only, assimilation still uses difference of observed and predicted soil moisture.

The above method is called nudging to gridded analysis and is meant for assimilating observations that are interpolated onto the problem grid. In the case observations are not interpolated but still closely related, another formulation called nudging to individual observations is preferred [45]:

$$\frac{\partial\theta}{\partial t} = \frac{\partial}{\partial x}\left(k(h)\frac{\partial h}{\partial x} - k(h)\right) - S_{\text{rwu}}(h,x,t) + G\,\frac{\sum_{i=1}^{N} W_i^2(x,t)\,\varepsilon(x)\left(\theta_i^{\text{obs}} - \theta\right)}{\sum_{i=1}^{N} W_i(x,t)}. \tag{14}$$

Equations (13), (14) present the general formulation of the NN. A number of improvements have been introduced to NN method in [30, 31, 46], some of which are discussed below.

3.1. Weighting functions

The weighting function $W(x,t)$ depends on the distance between the point of observation and running coordinates (x,t). In two-dimensional case, it can be separated into temporal and vertical weights,

$$W(x,t) = W_1(t)\, W_2(x). \tag{15}$$

These weights can be defined differently, and should be within the [0; 1] interval. Here we assume linear weight functions following [34]:

$$W_1(t) = \begin{cases} 1, & |t-t_0| \leqslant \frac{t_a}{2}; \\ \frac{t_a - |t-t_0|}{\frac{t_a}{2}}, & \frac{t_a}{2} < |t-t_0| < t_a; \\ 0, & |t-t_0| \geqslant t_a; \end{cases} \tag{16}$$

$$W_2(x) = \begin{cases} 1 - \frac{|x-x_0|}{R_x}, & |x-x_0| < R_x; \\ 0, & |x-x_0| < R_x. \end{cases} \tag{17}$$

Table 1. Values assigned to Newtonian nudging parameters.

Nudging parameter	Value
G	2.5 days^{-1}
ε	0.5
R_x	0.1 m
t_a	2 days

In the equations above t_a is active time, R_x is observation radius, t_0 and x_0 are time and depth of the observation, $x_0 = 0$ as for the surface observations. In our numerical experiments, we assumed these parameter values as presented in Table 1.

3.2. Nudging coefficient

The nudging factor G is meant to represent the relative magnitude of the nudging term to other processes. Original studies recommended to select it in the way that its time scale correspond to the slowest process in the model and, regarding the numerical stability condition, it is required that $G \leqslant 1/\Delta t$, where Δt is time step [45]. In [28], different scalar values of G are tested and the results are discussed. Nudging with constant G of both moisture and pressure heads is conducted in [31]. Optimal determination of nudging coefficient from adjoint equations is suggested in [47]. Later studies tend to treat G as a matrix rather than a scalar, similar to KF and 4D-Var matrices. For example, authors of [30] proposed to choose G from optimality conditions as either a scalar value or a matrix.

We considered the classical formulation of Newtonian nudging as in (13). However, our own numerical experiments with constant G proved unsatisfactory. Nudging effectively forced the solution to low moisture values, but performed poorly where moisture had to be pushed towards saturation. That is, the model readily predicted soil water shortage, but failed to consider sudden moisture rise, e.g. due to precipitation events underestimated or missed in the weather data. In cases soil water saturation was close to minimum, nudging often caused instabilities. Besides, the effect of assimilation varied between soil types, so the nudging coefficient had to be determined manually in each case. Therefore, we aimed to find a universal method to calculate G dynamically for any given soil characteristics.

The magnitude of terms in (11) depends on soil model parameters $\beta(h)$, hydraulic conductivity $k(h)$ and its derivative $v(h)$. We also find that, in the numerical scheme derived from the equation, the free term $\beta(h) \cdot h(x, t_{-1})$ occurs along with nudging term (here t_{-1} denotes time of the previous iteration). Another option is using a ratio of unsaturated and saturated soil water conductivities, $k(h)/k_0$. Both terms are dimensionless and represent the magnitude of terms in the moisture equation, so they can be used to weigh nudging coefficient. In our numerical experiments, we used the following combination of both:

$$G = 100 \left[\beta(h)\, |h| + 0.5 \frac{k(h)}{k_0} \right]. \tag{18}$$

Our numerical experiments suggest that this formulation works well for most soil types. However, it is purely empirical and lacks theoretical justification. Further tests are required to verify the formula.

4. Satellite moisture retrieval

The task of data assimilation needs low-noise and frequent satellite data. Active instruments on the Sentinel-1, RADARSAT, RISAT-1 and other satellites can provide high-resolution soil moisture data of around hundreds of meters with appropriate algorithms [48–50], but, as a rule, they have a sparse repeated interval around 10 days worldwide. Passive instruments on SMAP, AMSR-E, AMSR2 and SMOS. On the other hand, can provide high repeated interval worldwide of around a couple of days. However, without disaggregation algorithms [51,52], these instruments provide low resolution of around tens of kilometers. There are several algorithms to combine passive and active satellite data [53] but the temporary gaps have stayed unfilled.

To provide high-resolution soil moisture retrievals we applied disaggregation method to passive sensors AMSR-E, AMSR2 and SMAP to provide high resolution vertical and horizontal brightness temperature, land surface temperature for AMSR2 and AMSR-E data [54]. To calculate dielectric permittivity (DP) of the soil, we exploited Single Channel Algorithm — Vertical (SCA-V) [55] for SMAP disaggregated data and Land Parameter Retrieval Model for AMSR-E and AMSR2 data. It allows us to obtain DP maps with high resolution of 250×250 m, which is close to the field scale. We applied Mironov model for L-band [56] and Dobson model [57] for C-band to convert DP to soil moisture content.

5. Results of numerical experiments

It is a common approach to verify hydrological model results against the historical ground station data. Ground observations are often considered the most accurate measurements of soil moisture and provide independent benchmark to validate model simulations. Multiple ground station datasets are available in open access on the International Soil Moisture Network (ISMN) website [58].

For our study, we selected ground stations from the SCAN sensors network in USA, Arkansas, installed by the University of Arkansas at Pine Bluff (UAPB). The stations measure soil moisture and temperature on five layers: 5 cm, 10 cm, 20 cm, 50 cm and 100 cm, and also provide basic weather data such as precipitation and air temperature. Other weather parameters were downloaded from the ERA5 climate reanalysis database, which provides weather data at $0.25^\circ \times 0.25^\circ$ resolution grid [59]. As for the soil parameters, values for loamy soil were assumed. Simulations are conducted for the whole span of 2018. The initial conditions are assumed according to the satellite moisture estimates.

Here we present two kinds of validation tests. The first experiment is aimed to compare the performance of original Newtonian relaxation with scalar nudging coefficient (simulations are denoted NN) against dynamic variation described in section 3 (denoted DN). We evaluate results of both simulation experiments on every soil layer. The second experiment provides general small-scale assessment of the model performance and compares average result metrics for the selected ground stations.

Another, large-scale validation of the presented model was conducted in [60]. It involved data from all ISMN soil moisture stations located in the USA. However, due to the large difference of measurement approaches, the benchmark data were not uniform, and only surface measurements were considered. The experiment presented in this paper is more focused on the subsurface soil moisture and the effect of assimilating surface moisture observations on the root zone soil layers.

Model performance is evaluated by the means of the following key metrics: RMSE, bias, correlation (R) and index of agreement (IoA). The latter is defined as

$$\mathrm{IoA} = 1 - \frac{\sum_t \left(\theta^{\mathrm{DA}}(t) - \theta^{\mathrm{obs}}(t)\right)^2}{\sum_t \left(|\theta^{\mathrm{DA}}(t) - \overline{\theta^{\mathrm{obs}}(t)}| + |\theta^{\mathrm{obs}}(t) - \overline{\theta^{\mathrm{obs}}(t)}|\right)^2}. \tag{19}$$

For the second validation test, we also add assimilation efficiency coefficient (Eff) based on the improvement of MSE following [19]:

$$\text{Eff} = 100\% \left[1 - \frac{\sum_t \left(\theta^{\text{DA}}(t) - \theta^{\text{obs}}(t)\right)^2}{\sum_t \left(\theta^{\text{OL}}(t) - \theta^{\text{obs}}(t)\right)^2} \right]. \tag{20}$$

In the equations above, superscript 'obs' signifies observations to which result is compared (ground station measurements in our case), 'DA' — modeling with data assimilation, 'OL' — open-loop simulation.

5.1. One station experiment

First, we check the validity of the proposed dynamic nudging method. For that purpose, we run NN and DN simulation experiments for the selected ground station, *Lonoke Farm*. The rows of plots in Fig. 1 represent soil moisture on different soil layers on which moisture is measured by the ground station. The first plots, representing the top soil layer, also show the satellite retrieved moisture values.

As seen from the figure, satellite observations in general follow the trend of the ground station data. However, due to the imperfection of measurements, they contain noise and at times visibly diverge from the ground data. Model simulations, on the other side, are more constrained, so it can be noted that data assimilation mitigated the noise present in observations. Furthermore, comparison of simulation result plots demonstrates the problem with NN we noted above. Due to the constant G coefficient, relative force of nudging is not equal for various moisture levels, and so the nudging is noticeably 'weaker' at the periods when the soil is wetter. Notice that, although nudging is applied only to the top 10 cm of the problem domain, DN introduces improvement to all soil layers.

Table 2 presents the evaluation metrics for the single station experiment. RMSE is generally rather high for all soil layers. Positive bias indicates that the model is generally overestimating the soil moisture, especially on the topmost and the deepest soil layers. It can be mostly attributed to the imprecise choice of soil water retention parameters. Large errors on the top layer might be attributed to noisy forcing, and also difficulty of representing near-surface processes by the model.

Table 2. Summary of model performance evaluation for UAPB *Lonoke Farm* station by soil layers. Here NN stands for experiments with original Newtonian nudging formulation and DN — for proposed dynamical nudging method.

Depth	Experiment	RMSE	Bias	R	IoA
5 cm	NN	0.1104	0.0950	0.8571	0.7436
	DN	0.0714	0.0416	0.8653	0.8951
10 cm	NN	0.0696	0.0403	0.8349	0.8359
	DN	0.0595	0.0145	0.8504	0.9138
20 cm	NN	0.0785	0.0647	0.8073	0.7430
	DN	0.0567	0.0082	0.8380	0.8896
50 cm	NN	0.0899	0.0690	0.8695	0.7601
	DN	0.0435	0.0085	0.9053	0.9474
100 cm	NN	0.1205	0.1086	0.8241	0.6582
	DN	0.0608	0.0458	0.8996	0.8908
Average	NN	0.0938	0.0755	0.8386	0.7481
	DN	0.0584	0.0237	0.8717	0.9073

Nevertheless, other metrics indicate the plausible performance of the model as for a remote experiment. Correlation is very high on each layer, indicating the model is closely imitating the process dynamics. The index of agreement, as a complex indicator, is less favorable where RMSE is low, but still suggests the model is performing reasonably well in this case. Overall, better convergence is observed on the root zone layers, which is explained by the factors mentioned above. The best results are obtained for the 10 cm soil layer on this station, as well as on the most of other stations.

Comparison of evaluation metrics for the variants of nudging indicate relevant improvements in DN. Despite correlation is nearly unchanged and index of agreement only slightly increased, RMSE becomes considerably better due to lower bias. In general, simulation results fit closely to ground station data with average correlation of 0.87 and agreement of 0.90, although the bias at the top and bottom soil layers exceeds 0.04 in moisture units, which is relatively high.

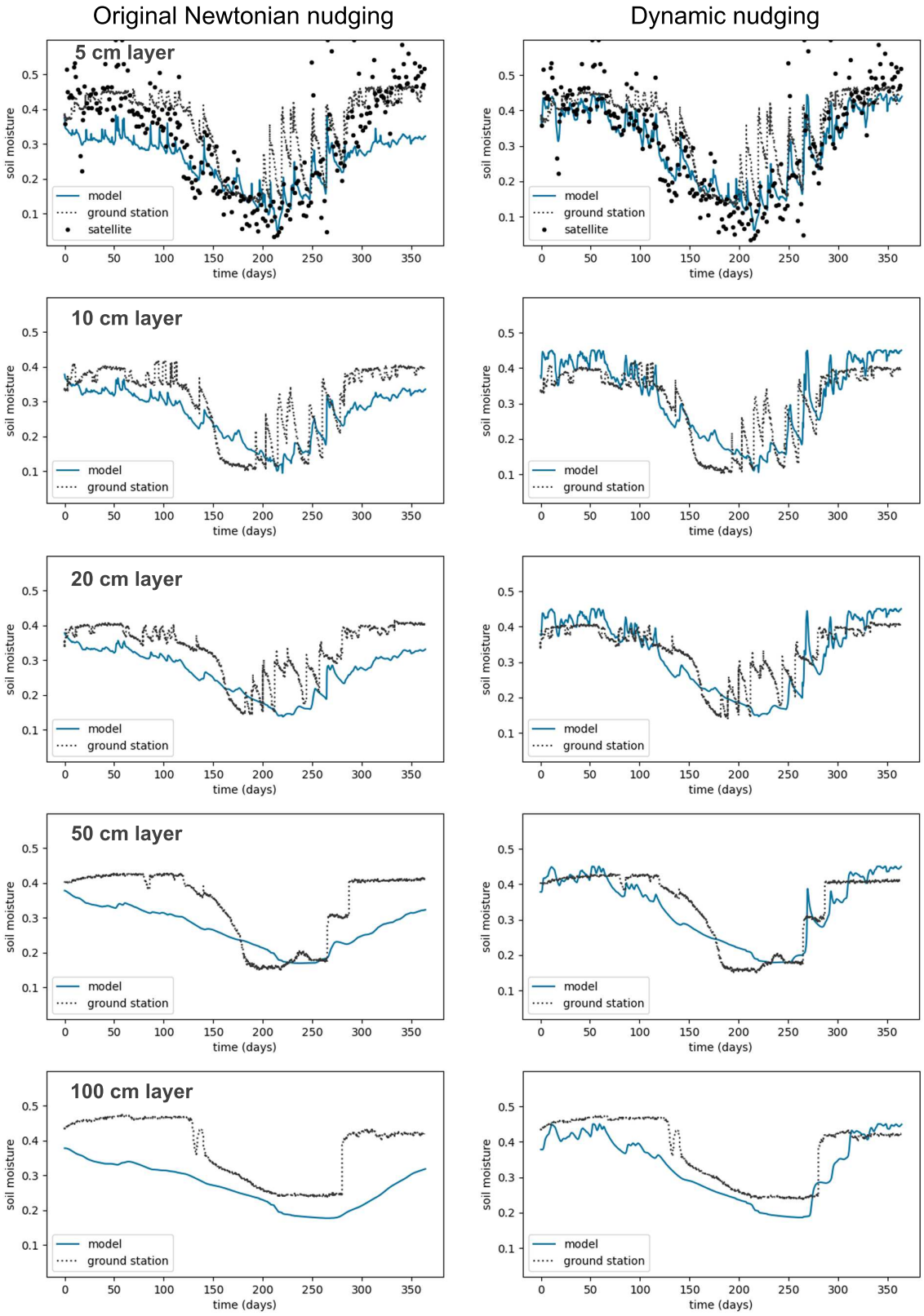

Fig. 1. Results of historical soil moisture calculation as compared to the ground station data on four soil levels. Left are simulations with constant G, right — with dynamically calculated G. Solid line represents model analysis, dotted line — ground station observations, single black dots — satellite observations.

5.2. Multiple stations experiment

For the general validation test, we calculate the same metrics plus assimilation efficiency for five UAPB ground stations. Table 3 shows the performance of the open loop, NN and DN experiments averaged over the ground measurement stations. Results indicate that open loop simulations are not estimating the state of the system accurately enough. However, as suggested by the theory, data assimilation succeeded in improving the model performance in every aspect. RMSE is considerably decreased with assimilation, from the average 0.1096 to 0.0818 and 0.0693 depending on the assimilation method, and bias is likewise decreased from 0.0703 to 0.0508 and 0.0329. Here, as in the previous case, our dynamic nudging method proved to be more flexible and accurate than the one with constant coefficient.

Table 3. Summary of model performance evaluation for UAPB soil moisture stations by soil layers. Here OL stands for open loop simulations, NN and DN are as in Table 2.

Station	Experiment	RMSE	Bias	R	IoA	Eff
5 cm	OL	0.1172	0.0797	0.5852	0.5436	—
	NN	0.0787	0.0565	0.8636	0.7920	54.32%
	DN	0.0579	0.0230	0.8451	0.9019	75.80%
10 cm	OL	0.1005	0.0601	0.4957	0.4976	—
	NN	0.0625	0.0286	0.6924	0.7301	61.76%
	DN	0.0588	0.0175	0.6913	0.7963	65.42%
20 cm	OL	0.1079	0.0498	0.4669	0.4033	—
	NN	0.0788	0.0301	0.7616	0.6824	47.41%
	DN	0.0708	0.0273	0.7481	0.7976	56.31%
50 cm	OL	0.1367	0.0914	0.3938	0.3305	—
	NN	0.1096	0.0696	0.5736	0.4456	30.91%
	DN	0.0873	0.0439	0.5281	0.5682	51.54%
100 cm	OL	0.0856	0.0705	0.2305	0.2697	—
	NN	0.0795	0.0694	0.0716	0.2801	17.77%
	DN	0.0716	0.0528	0.0992	0.3291	21.92%
Average	OL	0.1096	0.0703	0.4344	0.4089	—
	NN	0.0818	0.0508	0.5926	0.5860	42.44%
	DN	0.0693	0.0329	0.5824	0.6786	54.20%

The correlation on the 5 cm, 10 cm and 20 cm soil layers is also significantly improved by assimilation, as well as the index of agreement. Again, correlation is only slightly affected by the nudging method. Nevertheless, the assimilation efficiency indicates positive influence of assimilation in general (with average efficiency on all soil layers of 42.44%) and of the dynamical nudging approach in particular (efficiency of 54.2%). Note that, while the efficiency is almost equal on the 10 cm layer (61.76% against 65.42%), on the 5 cm layer the difference becomes considerable (54.32% against 75.8%).

On the deepest soil levels, correlation and agreement is weak due to observed influence of groundwater. The model calculates moisture based on the atmosphere and surface conditions, whereas deep layer soil moisture mostly depends on groundwater conditions which are currently not accounted for in the model. As seen from Table 2, where correlation with *Lonoke Farm* station data is rather high for all soil layers, surface information is enough for cases with low groundwater influence. In other cases, good correlation cannot be achieved without additional data. Nevertheless, values of RMSE and bias indicate that simulated results show reasonably good convergence with the ground station measurements.

6. Conclusions

In this study, we built a soil moisture simulation system that includes satellite image processing and the land model. Disaggregation algorithm provides high-resolution soil moisture maps, allowing the system to run precise simulations on the field scale.

Also, a dynamical variation of the Newtonian nudging method was proposed. The refined nudging coefficient is calculated based on physical soil parameters that are already present in the soil moisture equation. Compared to the use of constant nudging coefficient, it increases its variability and can provide improvement to simulation results. On the other hand, the proposed method is much more computationally cheap than optimal 4D analysis models, since it does not require solving additional problem.

Results of validation on UAPB SCAN ground stations were satisfactory for the whole one-meter-thick soil layer. Best convergence was found on the 10 cm layer. Assimilation efficiency increased from 42.44% to 54.2% in average due to the use of proposed nudging formulation. Correlation was mostly not affected, RMSE and the index of agreement improved by more than 15% in general. Our further publications will explore other assimilation approaches and model use cases, such as rainfall identification and irrigation planning. Also, an integration with crop growth model is planned for a more detailed account of crop factors, which would present a more clear practical usage of the model on a field scale.

[1] Paulik C., Dorigo W., Wagner W., Kidd R. Validation of the ASCAT Soil Water Index using in situ data from the International Soil Moisture Network. International Journal of Applied Earth Observation and Geoinformation. **30**, 1–8 (2014).

[2] Kedzior M.; Zawadzki J. Comparative study of soil moisture estimations from SMOS satellite mission, GLDAS database, and cosmic-ray neutrons measurements at COSMOS station in Eastern Poland. Geoderma. **283**, 21–31 (2016).

[3] Mishra V., Ellenburg W. L., Markert K. N., Limaye A. S. Performance evaluation of soil moisture profile estimation through entropy-based and exponential filter models. Hydrol. Sci. J. **65** (6), 1036–1048 (2020).

[4] Tian Y., Xiong L., Bin X., Zhuang R. A prior estimation of the spatial distribution parameter of soil moisture storage capacity using satellite-based root-zone soil moisture data. Remote Sens. **11**, 1–23 (2019).

[5] Guo Z., Dirmeyer P. A. Evaluation of the Second Global Soil Wetness Project soil moisture simulations: 1. Intermodel comparison. J. Geophys. Res. **111**, D22S02 (2006).

[6] Shellito P. J., Small E. E., Cosh M. H. Calibration of Noah soil hydraulic property parameters using surface soil moisture from SMOS and Basinwide in situ observations. J. Hydrometeor. **17**, 2275–2292 (2016).

[7] Yang K., Zhu L., Chen Y., Zhao L., Qin J., Lu H., Tang W., Han M., Ding B., Fang N. Land surface model calibration through microwave data assimilation for improving soil moisture simulations. Journal of Hydrology. **533**, 266–276 (2016).

[8] Jian Z., Huan Q., Li G., Li G. Parameters estimation and prediction of water movement and solute transport in layered, variably saturated soils using the ensemble Kalman Filter. Water. **11** (7), 1520 (2019).

[9] Chen W., Shen H., Huang C., Li X. Improving soil moisture estimation with a dual ensemble Kalman smoother by jointly assimilating AMSR-E brightness temperature and MODIS LST. Remote Sens. **9**, 273 (2017).

[10] Houser P. R., de Lannoy G. J. M., Walker J. P. Hydrologic data assimilation. In: Tiefenbacher, J. (Ed.) Approaches to Managing Disaster — Assessing Hazards, Emergencies and Disaster Impacts, pp. 41–64. IntechOpen (2012).

[11] Nearing G., Yatheendradas S., Crow W., Zhan X., Liu J., Chen F. The efficiency of data assimilation. Water Resour. Res. **54** (9), 6374–6392 (2018).

[12] Reichle R. H., Koster R. D., Liu P., Mahanama S. P. P., Njoku E. G., Owe M. Comparison and assimilation of global soil moisture retrievals from the Advanced Microwave Scanning Radiometer for the Earth Observing System (AMSR-E) and the Scanning Multichannel Microwave Radiometer (SMMR). J. Geophys. Res. **112**, D09108 (2007).

[13] Musuuza J. L., Gustafsson D., Pimentel R., Crochemore L., Pechlivanidis I. Impact of satellite and in situ data assimilation on hydrological predictions. Remote Sens. **12** (5), 811 (2019).

[14] Reichle R. H., Crow W. T., Koster R. D., Sharif H., Mahanama S. P. P. The contribution of soil moisture retrievals to land data assimilation products. Geophys. Res. Lett. **35**, L01404 (2008).

[15] Dong J., Crow W., Reichle R., Liu Q., Lei F., Cosh M. A global assessment of added value in the SMAP Level-4 soil moisture product relative to its baseline land surface model. Geophys. Res. Lett. **46**, 6604–6613 (2019).

[16] Rodell M., Houser P. R., Jambor U. E. A., Gottschalck J., Mitchell K., Meng C., Arsenault K., Cosgrove B., Radakovich J., Bosilovich M., Entin J. K., Walker J. P., Lohmann D., Toll D. The Global Land Data Assimilation System. Bulletin of American Meteorological Society. **85**, 381–394 (2004).

[17] Rains D., Han X., Lievens H., Montzka C., Verhoest N. E. C. SMOS brightness temperature assimilation into the Community Land Model. Hydrol. Earth Syst. Sci. **21**, 5929–5951 (2017).

[18] Dan B., Zheng X., Wu G., Li T. Assimilating shallow soil moisture observations into land models with a water budget constraint. Hydrol. Earth Syst. Sci. **24** (11) 5187–5201 (2020).

[19] Brocca L., Moramarco T., Melone F., Wagner W., Hasenauer S., Hahn S. Assimilation of surface- and root-zone ASCAT soil moisture products into rainfall–runoff modeling. IEEE Transactions on Geoscience and Remote Sens. **50** (7), 2542–2555 (2012).

[20] Bonan B., Albergel C., Zheng Y., Barbu A. L., Fairbairn D., Munier S., Calvet J. S. An ensemble square root filter for the joint assimilation of surface soil moisture and leaf area index within the Land Data Assimilation System LDAS-Monde: application over the Euro-Mediterranean region. Hydrol. Earth Syst. Sci. **24**, 325–347 (2020).

[21] Hostache R., Rains D., Mallick K., Chini M., Pelich R., Lievens H., Fenicia F., Corato G., Verhoest N. E. C., Matgen P. Assimilation of SMOS brightness temperature into a large-scale distributed conceptual hydrological model. Hydrol. Earth Syst. Sci. **24** (10), 4793–4812 (2019).

[22] De Lannoy G. J. M., Reichle R. H. Assimilation of SMOS brightness temperatures or soil moisture retrievals into a land surface model. Hydrol. Earth Syst. Sci. **20**, 4895–4911 (2016).

[23] Kumar S., Peters-Lidard C., Mocko D., Reichle R., Liu Y., Arsenault K., Xia Y., Ek M., Riggs G., Livneh B., Cosh M. Assimilation of remotely sensed soil moisture and snow depth retrievals for drought estimation. J. Hydrometeor. **15**, 2446–2469 (2014).

[24] Lei F., Crow W., Kustas W., Dong J., Yang Y., Knipper Ky., Anderson M., Notarnicola C., Greifeneder F., Mckee L., Alfieri J., Hain C., Dokoozlian N. Data assimilation of high-resolution thermal and radar remote sensing retrievals for soil moisture monitoring in a drip-irrigated vineyard. Remote Sens. Environ. **239**, 111622 (2020).

[25] Pinnington E., Quaife T., Black E. Impact of remotely sensed soil moisture and precipitation on soil moisture prediction in a data assimilation system with the JULES land surface model. Hydrol. Earth Syst. Sci. **22**, 2575–2588 (2018).

[26] Mao Y., Crow W. T., Nijssen B. Dual state/rainfall correction via soil moisture assimilation for improved streamflow simulation: evaluation of a large-scale implementation with Soil Moisture Active Passive (SMAP) satellite data. Hydrol. Earth Syst. Sci. **24**, 615–631 (2020).

[27] Martens B., Miralles D. G., Lievens H., van der Schalie R., de Jeu R. A. M., Fernández-Prieto D., Beck H. E., Dorigo W. A., Verhoest N. E. C. GLEAM v3: satellite-based land evaporation and root-zone soil moisture. Geoscientific Model Development. **10**, 1903–1925 (2017).

[28] Paniconi C., Marrocu M., Putti M., Verbunt M. Newtonian nudging for a Richards equation-based distributed hydrological model. Advances in Water Resources. **26**, 161–178 (2003).

[29] Houser P. R., Shuttleworth W. J., Famiglietti J. S., Gupta H. V., Syed K. H., Goodrich D. C. Integration of soil moisture remote sensing and hydrologic modeling using data assimilation. Water Resour. Res. **34** (12), 3405–3420 (1998).

[30] Vidard A., le Dimet F. X., Piacentini A. Optimal determination of nudging coefficients. Tellus A. **55** (1), 1–15 (2003).

[31] Camporese M., Paniconi C., Putti M., Salandin P. Comparison of data assimilation techniques for a coupled model of surface and subsurface flow. Vadose Zone J. **8** (4), 837–845 (2009).

[32] Botto A., Belluco E., Camporese M. Multi-source data assimilation for physically based hydrological modeling of an experimental hillslope. Hydrol. Earth Syst. Sci. **22**, 4251–4266 (2018).

[33] Bauser H. H., Berg D., Klein O., Roth K. Inflation method for ensemble Kalman filter in soil hydrology. Hydrol. Earth Syst. Sci. **22**, 4921–4934 (2018).

[34] Miroslaw-Swiatek D. Application of Newtonian nudging data assimilation method in hydrodynamic model of flood flow in the lower Biebrza basin. Studia Geotechnica et Mechanica. **34** (2), 91–105 (2012).

[35] Saito H., Šimůnek J., Mohanty B. Numerical analyses of coupled water, vapor and heat transport in the vadose zone. Vadose Zone J. **5** (2), 784–800 (2006).

[36] Šimůnek J., van Genuchten M. Th., Sejna M. The HYDRUS software package for simulating two- and three dimensional movement of water, heat, and multiple solutes in variably-saturated porous media. Technical manual; version 2.0. PC Progress (2012).

[37] Gebler S., Kurtz W., Pauwels V. R. N., Kollet S. J., Vereecken H., Franssen H. J. Assimilation of high-resolution soil moisture data into an integrated terrestrial model for a small-scale head-water catchment. Water Resour. Res. **55**, 10358–10385 (2019).

[38] Philip J. R., de Vries D. A. Moisture movement in porous materials under temperature gradients. Eos, Transactions of the American Geophysical Union. **38** (2), 222–232 (1957).

[39] Schaap M. G., van Genuchten M. Th. A modified Mualem–van Genuchten formulation for improved description of the hydraulic conductivity near saturation. Vadose Zone J. **5**, 27–34 (2005).

[40] Zhang Y., Schaap M. G. Weighted recalibration of the Rosetta pedotransfer model with improved estimates of hydraulic parameter distributions and summary statistics (Rosetta3). Journal of Hydrology. **547**, 39–53 (2017).

[41] Sadeghi M., Ghanbarian B., Horton R. Derivation of an explicit form of the percolation-based effective-medium approximation for thermal conductivity of partially saturated soils. Water Resour. Res. **54**, 1389–1399 (2018).

[42] Xu C.-Y., Singh V. P. Cross comparison of empirical equations for calculating potential evapotranspiration with data from Switzerland. Water Resources Management. **16**, 197–219 (2002).

[43] Feddes R. A., Kowalik P. T., Zaradny H. Simulation of field water use and crop yield. Pudoc (1978).

[44] Samarskiy A. A. The theory of difference schemes. Marcel Dekker (2001).

[45] Stauffer D. R., Seaman N. L. Multiscale four-dimensional data assimilation. Journal of Applied Meteorology. **33**, 416–434 (1994).

[46] Auroux D., Nodet M. The back and forth nudging algorithm for data assimilation problems: theoretical results on transport equations. ESAIM: Control, Optimisation and Calculus of Variations. **18**, 318–342 (2012).

[47] Stauffer D. R., Bao J. W. Optimal determination of nudging coefficients using the adjoint equations. Tellus A: Dynamic Meteorology and Oceanography. **45** (5), 358–369 (1993).

[48] Paloscia S., Pettinato S., Santi E., Notarnicola C., Pasolli L., Reppucci A. Soil moisture mapping using Sentinel-1 images: Algorithm and preliminary validation. Remote Sens. Environ. **134**, 234–248 (2013).

[49] Merzouki A., McNairn H., Pacheco A. Mapping soil moisture using RADARSAT-2 data and local autocorrelation statistics. IEEE J. Selected Topics Appl. Earth Obs. Remote Sens. **4** (1), 128–137 (2011).

[50] Ponnurangam G. G., Jagdhuber T., Hajnsek I., Rao Y. S. Soil moisture estimation using hybrid polarimetric SAR Data of RISAT-1. IEEE Transactions on Geoscience and Remote Sens. **54** (4), 2033–2049 (2016).

[51] Chaubell J., Yueh S., Entekhabi D., Peng J. Resolution enhancement of SMAP radiometer data using the Backus Gilbert optimum interpolation technique. 2016 IEEE International Geoscience and Remote Sensing Symposium (IGARSS). 284–287 (2016).

[52] Poe G. A. Optimum interpolation of imaging microwave radiometer data. IEEE Transactions on Geoscience and Remote Sens. **28** (5), 800–810 (1990).

[53] Das N. N., Entekhabi D., Scott Dunbar R., Chaubell M. J., Colliander A., Yueh S., Jagdhuber Th., Chen F., Crow W., O'Neill P. E., Walker J. P., Berg A., Bosch D. D., Caldwell T., Cosh M. H., Collins Ch. H., Lopez-Baeza E., Thibeault M. The SMAP and Copernicus Sentinel 1A/B microwave active-passive high resolution surface soil moisture product. Remote Sens. Environ. **233**, 111380 (2019).

[54] Holmes T. R. H., de Jeu R. A. M., Owe M., Dolman A. J. Land surface temperature from Ka band (37 GHz) passive microwave observations. J. Geophys. Res. **114**, D04113 (2009).

[55] Chan S., Bindlish R., O'Neill P., Njoku E., Jackson T., Colliander A., Chen F., Burgin M., Dunbar S., Piepmeier J., Yueh S., Entekhabi D., Cosh M., Caldwell T., Walker J., Wu X., Berg A., Rowlandson T.,

Pacheco A., Kerr Y. Assessment of the SMAP Passive Soil Moisture Product. IEEE Transactions on Geoscience and Remote Sens. **54**, 1–14 (2016).

[56] Mironov V. L., Kerr Y., Wigneron J.-P., Kosolapova L., Demontoux F. Temperature- and texture-dependent dielectric model for moist soils at 1.4 GHz. IEEE Geoscience and Remote Sensing Letters. **10**, 419–423 (2013).

[57] Peplinski N. R., Ulaby F. T., Dobson M. C. Dielectric properties of soils in the 0.3-1.3-GHz range. IEEE Transactions on Geoscience and Remote Sens. **33** (3), 803–807 (1995).

[58] Dorigo W., Wagner W., Hohensinn R., Hahn S., Paulik C., Xaver A., Gruber A., Drusch M., Mecklenburg S., Oevelen P., Robock A., Jackson T. The International Soil Moisture Network: a data hosting facility for global in situ soil moisture measurements. Hydrol. Earth Syst. Sci. **15**, 1675–1698 (2011).

[59] Hersbach H., de Rosnay P., Bell B., Schepers D., Simmons A., Soci C., Abdalla S., Alonso-Balmaseda M., Balsamo G., Bechtold P., Berrisford P., Bidlot J.-R., de Boisseson E., Bonavita M., Browne P., Buizza R., Dahlgren P., Dee D., Dragani R., Diamantakis M., Flemming J., Forbes R., Geer A. J., Haiden T., Holm E., Haimberger L., Hogan R., Horanyi A., Janiskova M., Laloyaux P., Lopez P., Munoz-Sabater J., Peubey C., Radu R., Richardson D., Thepaut J.-N., Vitart F., Yang X., Zsoter E., Zuo H. Operational global reanalysis: progress, future directions and synergies with NWP. ERA Report 27 (2018).

[60] Kozhushko O., Boiko M., Kovbasa M., Martyniuk P., Stepanchenko O., Uvarov M. Evaluation of the soil moisture model with data assimilation by the triple collocation method. Modeling, Control and Information Technologies: Proceedings of International Scientific and Practical Conference. **4**, 35–38 (2020).

Комп'ютерне моделювання вологості ґрунту на рівні поля із використанням динамічного алгоритму релаксації

Кожушко О. Д.[1,2], Бойко М. В.[1,2], Ковбаса М. Ю.[3],
Мартинюк П. М.[1,2], Степанченко О. М.[1,2], Уваров М. В.[1,4]

[1]*EOS Data Analytics,*
пров. Десятинний, 5, 01025, Київ, Україна
[2]*Національний університет водного господарства та природокористування,*
вул. Соборна, 11, 33028, Рівне, Україна
[3]*Інститут фізики напівпровідників ім. В. Є. Лашкарьова НАН України,*
просп. Науки, 41, 03028, Київ, Україна
[4]*Інститут металофізики ім. Г. В. Курдюмова НАН України,*
бул. Академіка Вернадськкого, 36, 03142, Київ, Україна

Оцінки вологості ґрунту широко використовуються у численних практичних задачах, від прогнозу погоди до точного землеробства. В останні роки доступність даних про вологість зросла завдяки стрімкому розвитку алгоритмів обробки супутникових зображень. Проте, більшість отриманих даних із супутників відображають лише поверхневу вологість із недостатньо високою роздільною здатністю. У цій роботі ставимо за мету відновити поверхневу вологість ґрунту на рівні поля завдяки використанню алгоритмів декомпозиції. Крім того, використовуємо математичну модель на основі рівняння Річардса для оцінки вологості ґрунту в кореневій зоні. Результати обох моделей поєднуються завдяки алгоритму асиміляції даних, що називається ньютонівською релаксацією. Запропонована динамічна варіація методу, яка полегшує його адаптацію до різних типів ґрунту та покращує результати моделювання. Проведено два типи чисельних експериментів. Результати комп'ютерних симуляцій узгоджуються із реальними даними з достатньою точністю. Загалом, отримана модель показує кореляцію 0.58 на всій кореневій зоні, досягаючи 0.85 на приповерхневих шарах ґрунту.

Ключові слова: *асиміляція даних, дистанційне зондування Землі, алгоритм ньютонівської релаксації, комп'ютерне моделювання, супутникове відновлення вологості, вологість ґрунту.*